Biosensors and Bioelectronics 43 (2013) 173–179

Contents lists available at SciVerse ScienceDirect

Biosensors and Bioelectronics

journal homepage: www.elsevier.com/locate/bios

rGO/SWCNT composites as novel electrode materials for electrochemical biosensing

Tzu-Yen Huang [a,b], Jen-Hsien Huang [b], Hung-Yu Wei [b,c], Kuo-Chuan Ho [a,c,*], Chih-Wei Chu [b,d,**]

[a] Department of Chemical Engineering, National Taiwan University, Taipei (R.O.C.) 10617, Taiwan
[b] Research Center for Applied Sciences, Academia Sinica, Taipei (R.O.C.) 11529, Taiwan
[c] Institute of Polymer Science and Engineering, National Taiwan University, Taipei (R.O.C.) 10617, Taiwan
[d] Department of Photonics, National Chiao-Tung University, Hsinchu (R.O.C.) 30010, Taiwan

ARTICLE INFO

Article history:
Received 28 July 2012
Received in revised form
13 October 2012
Accepted 15 October 2012
Available online 23 November 2012

Keywords:
Single-walled carbon nanotubes
Graphene oxide
Sensors
Hydrogen peroxide
β-Nicotinamide adenine dinucleotide

ABSTRACT

In this study we performed electrochemical sensing using conductive carbon composite films containing reduced graphene oxide (rGO) and single-walled carbon nanotubes (SWCNTs) as electrode modifiers on glassy carbon electrodes (GCEs). Raman spectroscopy, transmission electron microscopy, atomic force microscopy, and scanning electron microscopy all suggested that the rGO acted as a surfactant, covering and smoothing out the surface, and that the SWCNTs acted as a conducting bridge to connect the isolated rGO sheets, thereby (i) minimizing the barrier for charge transfer between the rGO sheets and (ii) increasing the conductivity of the film. We used the rGO/SWCNT–modified GCE as a sensor to analyze hydrogen peroxide (H_2O_2) and β-nicotinamide adenine dinucleotide (NADH), obtaining substantial improvements in electrochemical reactivity and detection limits relative to those obtained from rGO- and SWCNT-modified electrodes, presumably because of the higher conductivity and greater coverage on the GCE, due to π–π interactions originating from the graphitic structures of the rGO and SWCNTs. The electrocatalysis response was measured by cyclic voltammetry and amperometric current–time (*i*–*t*) curve techniques. The linear concentration range of H_2O_2 and NADH detection at rGO/SWCNT–modified electrode is 0.5–5 M and 20–400 μM. The sensitivity for H_2O_2 and NADH detection is 2732.4 and 204 μA mM^{-1} cm^{-2}, and the limit of detection is 1.3 and 0.078 μM respectively. Furthermore, interference tests indicated that the carbon composite film exhibited high selectivity toward H_2O_2 and NADH. Using GO as a solubilizing agent for SWCNTs establishes a new class of carbon electrodes for electrochemical sensors.

1. Introduction

Carbon nanotubes (CNTs)—one-dimensional carbon materials with remarkable electrical, chemical, structural, and mechanical properties—are attracting enormous interest for their practical applications,(Wang et al., 2004; Zhu et al., 2007; Chen et al., 2011) particularly as electrode materials in electrochemical sensors, which benefit greatly from their ability to promote electron-transfer reactions, their highly accessible surface area, and their excellent biochemical stability.[Guldi et al., 2005; Daniel et al., 2007; Lin et al., 2004; Callegari et al., 2004; Karyakin et al., 1999) Inherent insolubility in solvents, particular water, is, however, a major barrier for developing the biomedical applications and biophysical processing of CNTs. Both covalent and noncovalent functionalization have been used to stabilize CNTs in aqueous media to address the challenge of solubilizing them for applications in biosensor technologies. For covalent modification, CNTs are usually treated under extreme oxidative conditions,(Li et al., 2009; Manjunatha et al., 2011; You et al., 2011; Yang and Zhang, 2011; Abbaspour and Noori, 2011; Si et al., 2011) resulting in the ends and side walls becoming rich in oxygenated functions—mainly carboxyl groups. Because a significant portion of the π-electronic network is destroyed, it may be difficult to break the CNTs or even to shorten them, severely impairing their intrinsic electronic properties. Hence, noncovalent functionalization, which disperses CNTs in aqueous based on van der Waals forces or π-stacking interactions without destroying their electronic structure, is an attractive process, often facilitated by polymers or surfactants.(Kruusenberg et al., 2009; Rubianes and Rivas, 2007; Guo et al., 2011; Leng et al.,2011) Nevertheless, the poor electronic properties of polymers and surfactants remaining on the electrode surface can comprise the

* Corresponding author at: Department of Chemical Engineering, National Taiwan University, Taipei (R.O.C.) 10617, Taiwan.
Tel.: +886 2 23660739; fax: +886 2 23623040.
** Corresponding author at: Research Center for Applied Sciences, Academia Sinica, Taipei (R.O.C.) 11529, Taiwan.
Tel.: +886-2-27898000 × 270; fax: +886 2 27826680.
E-mail addresses: kcho@ntu.edu.tw (K.-C. Ho), gchu@gate.sinica.edu.tw (C.-W. Chu).

0956-5663/$ - see front matter © 2012 Elsevier B.V. All rights reserved.
http://dx.doi.org/10.1016/j.bios.2012.10.047

performance of the electrochemical sensors, resulting in poor accuracy. Accordingly, developing suitable materials for the aqueous dispersion of CNTs, while maintaining their properties, remains a challenge for noncovalent solubilization approaches.

Graphene oxide (GO) consists of a single atomic layer of sp^2-hybridized carbon atoms functionalized with mainly phenol, hydroxyl, and epoxide groups on the basal plane and ionizable carboxyl groups at the edges; it is obtained after treating graphite with strong oxidizers. Because of charge repulsion of the ionized edge acid groups, GO forms stable single-layer aqueous dispersions. As a derivatized graphite nanomaterial, GO features a highly hydrophobic surface with non-oxidized polyaromatic nanographene domains on the basal plane. The abundance of highly conjugated structures on the surface of GO allows it to adhere readily to conjugated materials through π–π interactions, making GO function as a unique tethered 2D surfactant sheet. (Geim and Novoselov, 2007; Parpia et al., 2007; Gilje et al., 2007; Schedin et al., 2007; Tung et al., 2011; Huang et al., 2010).

The detection of hydrogen peroxide (H_2O_2) has drawn increasing attention in recent years. Because H_2O_2 is the product of reactions catalyzed by selective oxidase enzymes (Safavia and Farjamia, 2011; Dey and Raj, 2010] and an essential compound widely used in clinical, food, pharmaceutical and environmental fields [Chena et al., 2012). Dihydronicotinamide adenine dinucleotide (NADH) and its oxidized form, nicotinamide adenine dinucleotide (NAD^+), are the main charge carriers in cells. The electrochemical oxidation of NADH has received considerable interest because of its significance both as a cofactor for dehydrogenase enzymes and its role in the electron-transfer chain in biological systems (Sun et al., 2012).

Recently, many studies have confirmed that GO is a good candidate for use as an advanced carbon material in electrochemical applications.(Deng et al., 2011; Ge et al., 2012) Because CNTs and GO exhibit many similar properties, while being structurally dissimilar, the noncovalent preparation of rGO/CNT composites provides attractive building blocks for the development of nanocarbon materials with potentially improved conductivity and catalytic ability for electrochemical research. Here, we prepared rGO/single-walled carbon nanotube (SWCNT) composites through a surfactant-free method and then use them as modifiers on glassy carbon electrodes (GCEs) for electrochemical sensing applications. By comparing the electrochemical performance of the carbon composite films with those of its individual constituents, we found that the rGO/SWCNT films exhibited much better electrochemical and electrocatalytic activities toward tested analytes, attributable to the synergistic effects of the rGO and SWCNTs. Furthermore, interference tests of the composite films also revealed high selectivity toward the tested analytes. Thus, rGO/SWCNT composite films can be used to develop novel types of highly sensitive and stable electrochemical sensors.

2. Experimental

2.1. Chemicals

Graphite powder (Bay Carbon, SP-1), SWCNTs, ascorbic acid (AA), dopamine (DA), uric acid (UA), L-cysteine (L-cys), β-nicotinamide adenine dinucleotide (NADH), and hydrogen peroxide (H_2O_2) were purchased from Sigma–Aldrich. All other chemicals were of analytical grade and used without further purification. Aqueous solutions were prepared using double distilled water. The supporting electrolyte for the electrochemical studies was 0.1 M phosphate buffer solution (PBS, pH 7), which was prepared from Na_2HPO_4 and NaH_2PO_4 solutions. All solutions were deoxygenated by purging with pre-purified N_2 gas.

2.2. Apparatus and measurement

Cyclic voltammetry (CV) was performed using a CHI 440 analytical system (CH Instruments) and its compatible software. A conventional three-electrode cell assembly, consisting of an Ag/AgCl reference electrode and a Pt wire counter electrode, was used for the electrochemical measurements. The working electrode was either an unmodified GCE or a GCE modified with a carbon (composite) film. All measurements were performed at 25 ± 2 °C. An alpha 300 Raman spectrometer (WITec Instruments, Germany) was used to analyze the chemical compositions of the carbon composite films, at a fixed wavelength of 514.5 nm. The surface morphologies of the carbon composite films were investigated using atomic force microscopy (AFM, Digital Instrument NS 3a controller equipped with a D3100 stage) and scanning electron microscopy (SEM, Hitachi S-4700).

2.3. Preparation of rGO/SWCNT-modified electrode

GO was prepared from graphite powder using a modified version of Hummers' method.(Hummers and Offeman, 1958) Briefly, graphite powder (2 g), $NaNO_3$ (1 g), and H_2SO_4 (46 mL) were mixed in an ice bath and then $KMnO_4$ (6 g) was added slowly. Once mixed, the solution was transferred to a water bath and stirred at 35 °C for approximately 1 h, forming a thick paste. Water (80 mL) was added and then the solution was stirred for 1 h at 90 °C. Finally, more water (200 mL) was added, followed by the slow addition of H_2O_2 (30%, 6 mL). The warm solution was filtered and washed sequentially with 10% HCl (3×200 mL2) and water (200 mL). The filter cake was dispersed in water through mechanical agitation and then stirred overnight. The dispersion was left to settle and the supernatant (clear yellow dispersion) subjected to dialysis for 1 month, resulting in a stock solution having a GO concentration of approximately 0.17 mg mL^{-1}. The stable dispersion was filtered through an alumina membrane and left to dry for several days. The GO paper was then carefully peeled from the filter and stored under ambient conditions. To produce hybrid suspensions of rGO and SWCNTs, dry powders of GO and SWCNTs were dispersed directly in anhydrous hydrazine and left to stir for 1 week. Hydrazine bubbled violently upon contact with the GO and SWCNT powders, but soon formed a uniform dark gray suspension with no visible precipitation. After mixing the materials with hydrazine solution, the dark gray suspension was centrifuged to separate out the residual SWCNT bundles and aggregated rGO. After centrifugation, the uniformity of the rGO/SWCNT dispersion was ensured through heating at 60 °C with repeated ultrasonic agitation for approximately 30 min. Typically, a mixture of GO (1 mg mL^{-1}) and SWCNTs (5 mg mL^{-1}) in hydrazine was employed to prepare a modified electrode.

Bare GCEs were used for modification. Before starting each experiment, GCEs were polished using a BAS polishing kit and a slurry of 0.05-μm aluminum oxide (Al_2O_3) powder and then rinsed sequentially with deionized water and EtOH. The GCEs were coated uniformly with an rGO/SWCNT dispersion (3 μL) and dried in an oven. The obtained rGO/SWCNT–modified GCEs were washed carefully in deionized water to remove residual carbon materials and solvent from the GCE, and then dried at room temperature.

3. Results and discussion

3.1. Characterization of rGO/SWCNT composite film

The signals from resonance Raman spectra reflected the degrees of stacking and functionality of the SWCNTs, GO, and rGO/SWCNT composites. Fig. 1 reveals signals for the SWCNTs at 1596 and 1587 cm^{-1}, associated with phonon transitions within

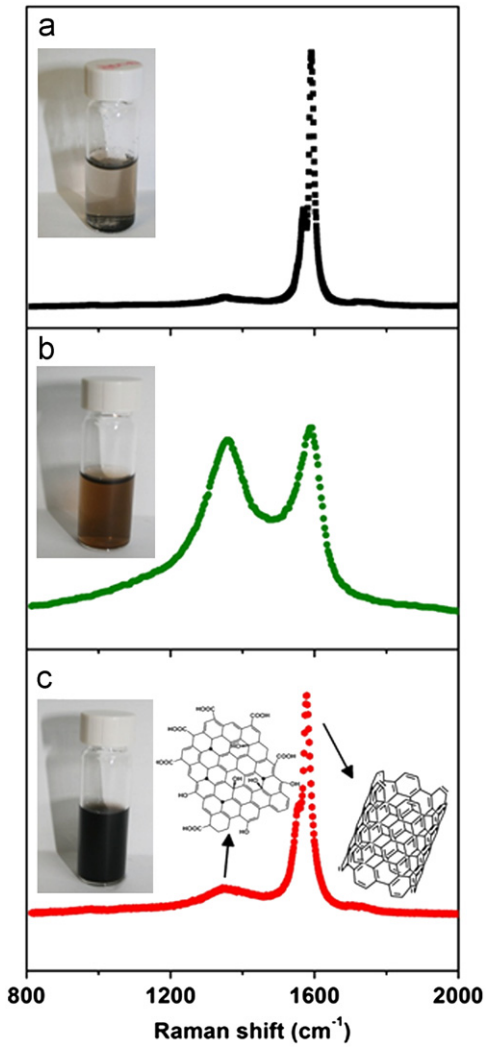

Fig. 1. Raman spectra of films of (a) SWCNTs, (b) GO, and (c) the rGO/SWCNTs composite.

the 1-D SWCNTs, and the D and G peaks of GO at 1350 and 1591 cm^{-1}, respectively. The D peak of rGO and the signals of the SWCNTs appeared in the spectrum of the hybrid film, indicating that the rGO and SWCNTs co-existed and maintained their individual electronic properties.

Fig. 2(a) and (b) display transmission electron microscopy (TEM) images of the carbon composite material. Each rGO sheet possessed a planar structure, like paper, with several monolayers stacked together. SWCNTs can form uniform solutions in hydrazine through the creation of hydrazinium compounds, comprising negatively charged SWCNTs surrounded by $N_2H_5^+$ counterions. (Mitzi et al., 2005; Tung et al., 2009) Nevertheless, the TEM image in Fig. 2(a) reveals serious aggregation, with many SWCNTs bundles. After sonicating with rGO for several hours, the rGO/SWCNT colloidal dispersion was stable for several months without visible precipitation, indicating that the rGO acted as a molecular surfactant to disperse the SWCNTs,(Cote et al., 2009; Kim et al., 2010) with the planar structure of rGO providing a large surface area for interaction with the SWCNTs. The highly conjugated structures on the rGO surface allowed it to adhere readily to the cylindrical planes of the SWCNTs. Fig. 2(b) displays a region of the surface of the rGO/SWCNT composite film; it reveals SWCNTs running across the rGO surface to form a conductive network.

To better understand the surface morphology and structural features, we used SEM to characterize the deposited composite. Fig. 2(c) and (d) present SEM images of an SWCNT film and an rGO/SWCNT composite film, respectively. Heavily entangled SWCNT bundles were present in the film of the pristine SWCNTs (Fig. 2(c)), resulting in non-uniform coverage across the substrate surface. In contrast, for the rGO/SWCNT composite film, Fig. 2(d) reveals that the SWCNTs were debundled and adhered to the rGO sheets, presumably through $\pi-\pi$ interactions of their graphitic structures. Although SEM images can be used to understand the general morphology of a film, they do not provide topographical information. Therefore, we employed AFM to establish the surface roughnesses of the deposited films. Fig. 2(e) and (f) present typical AFM images for the pristine SWCNT and hybrid rGO/SWCNT films, respectively. The hybrid film exhibits a much smoother surface [root mean square (rms) roughness = 5 nm] than that of the SWCNT film (rms roughness = 35 nm), indicating that the rGO acted as a blanket, covering the SWCNTs to smooth out the surface, with the SWCNTs acting as conductive bridges that connected the rGO sheets, thereby minimizing the barrier for charge transfer between the rGO sheets and decreasing the sheet resistance, consistent with the TEM images. This surfactant-free method for the dispersion of SWCNTs inspired us to further investigate their electrochemical behavior.

3.2. Electrochemical behavior of rGO/SWCNT composite film

We used cyclic voltammetry (CV) to investigate the electrochemical behavior of a bare GCE and electrodes modified with rGO, SWCNTs, and rGO/SWCNTs, recording at a scan rate of 100 mV s^{-1} in N_2-saturated PBS. Fig. 3(a) reveals that the unmodified (bare) GCE exhibited no obvious redox peaks in PBS at applied potentials between −0.6 and +0.6 V. On the other hand, the SWCNT- and rGO-only modified electrodes displayed redox couples, with formal potentials of −60 and 20 mV, respectively; the rGO/SWCNT–modified electrode also exhibited a well-defined redox couple with a formal potential of −40 mV and a coupling of the electrochemical properties contributed from both the rGO and the SWCNTs. Although the rGO exhibited excellent two-dimensional conducting properties, the gaps between isolated rGO layers impeded charge transfer, resulting in the formation of a barrier. This problem could be solved after blending the rGO with the SWCNTs. The SWCNTs acted as conductive bridges to connect the isolated rGO layers, thereby increasing the conductivity. Therefore, the rGO/SWNCTs hybrid displayed enhanced conductivity and electrochemical background, leading to rapid transfer of electrons and improved catalytic ability.

Fig. 3(b) displays the effect of the scan rate on the electrochemical behavior of the rGO/SWCNT film obtained from a neutral aqueous solution. The rGO/SWCNT–modified electrode exhibited higher stability with increasing scan rate; the plot of the peak currents (I_{pa} and I_{pc}) with respect to the scan rate in the inset to Fig. 3(b) reveals a linear dependence (R^2 = 0.998 and 0.994, respectively) and an I_{pa}/I_{pc} ratio of close to unity. This behavior is consistent with a reversible electron transfer process for scan rates between 50 and 500 mV s^{-1}. The peak currents of the redox couples are directly proportional to the scan rate, indicating that the redox process occurring at the rGO/SWCNT–modified electrode was that expected for a surface-confined process.

The reproducibility and stability is an important issue to characterize the bio-sensing system. For reproducibility, five repetitive measurements by cyclic voltammetry at five rGO/SWCNT-modified electrodes with same experimental procedure were carried out in 0.1 M neutral PBS solution and the background current variations of the rGO/SWCNT-modified electrodes were less than 2% which validate the reproducible process of rGO/SWCNT composite on the GCE surface. The results show that the

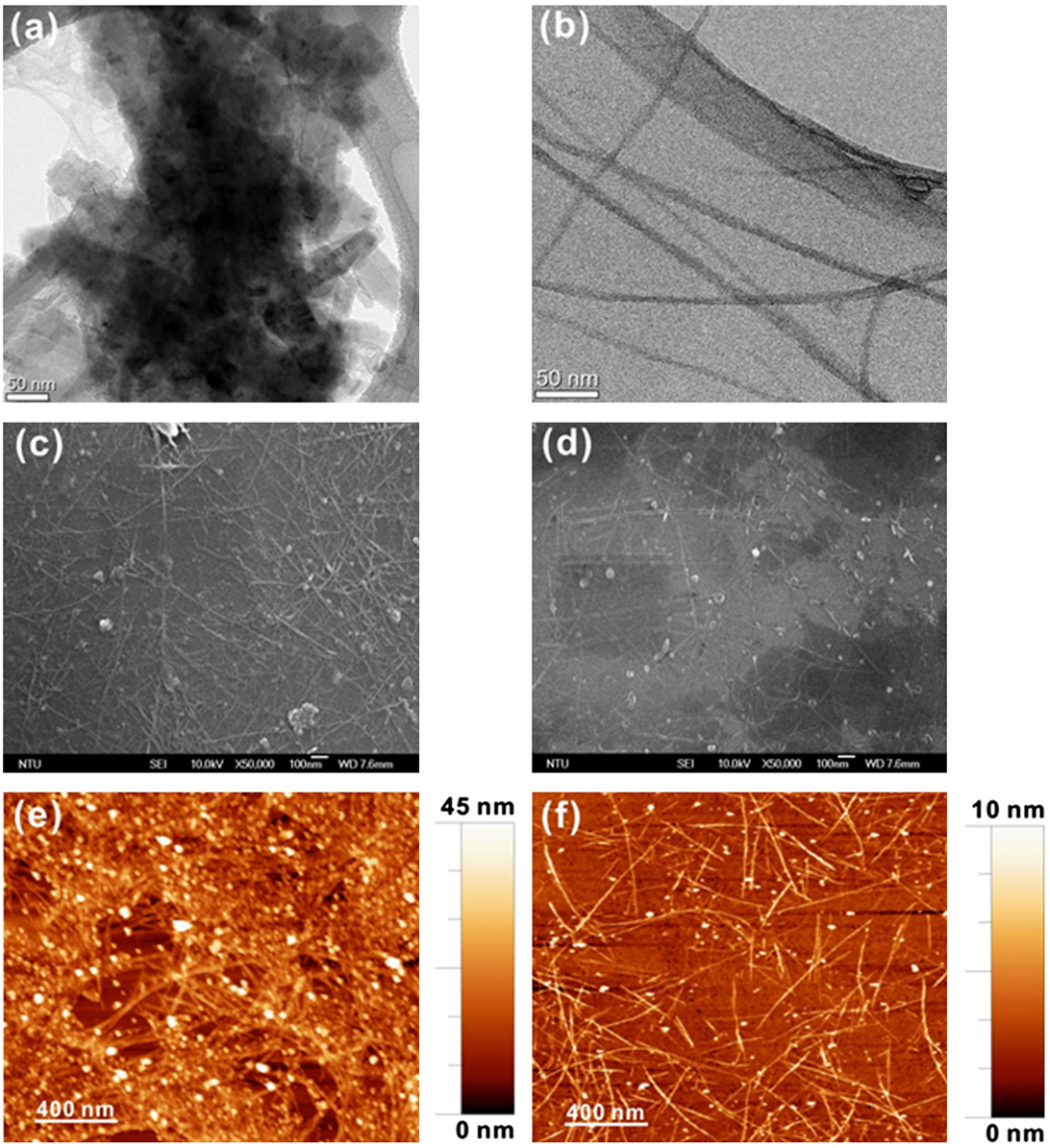

Fig. 2. TEM, SEM and AFM images of SWCNTs and rGO/SWCNTs. TEM images of (a) SWCNTs and (b) rGO/SWCNTs (dispersed solutions) at low-magnification (scale bar: 50 nm). The SWCNTs aggregated in solution, forming many bundles; rGO acted as a surfactant to disperse the SWCNTs; certain areas of the surface of the rGO featured many interacting SWCNTs. Corresponding SEM images (c, d). AFM images with height profiles of films of the (e) SWCNTs and (f) rGO/SWCNT composite. The AFM and SEM images reveal that rGO effectively debundled the SWCNTs.

fabrication process is reliable and the modified electrodes are reproducible. For stability, repetitive cyclic voltammetry experiment in 0.1 M neutral PBS solution to determine the stability for rGO/SWCNT-modified electrode. In Fig. 3(c), the results express that the peak current decreased less than 6% after 100 continuous scan cycles with 100 mV^{-1} scan rate. To further investigate the stability, we keep the rGO/SWCNT-modified electrode in the room temperature for 3 weeks and the current response decrease about 10% compared to the original current response, also indicating that the rGO/SWCNT-modified electrode has good storage stability.

To further characterize the rGO/SWCNT–modified electrode, we examined the effect of pH on the CV traces. After recording cyclic voltammograms of the rGO/SWCNTs on the GCE in PBS, we washed the system with deionized water and transferred it into aqueous buffer solutions at various values of pH (Fig. 4). The film was highly stable in the range between pH 1 and 13, with an obvious redox couple in each solution, suggesting a potential use for the rGO/SWCNT–modified electrode in pH sensing. In particular, the CV trace recorded under neutral conditions revealed a stable signal and a well-defined redox couple, suggesting that the system would be beneficial for analyte detection. The values of the peak potentials (E_{pa} and $E_{pc)}$ were dependent on the pH of the buffer solution. The inset to Fig. 4 plots the potential of the rGO/SWCNT composite with respect to the pH over the range from 1 to 13. We calculated the slope of the response shows to be 62 mV pH^{-1}, which is close to the theoretical value of 56 mV pH^{-1} from the Nernst equation for an equal number of proton and electron transfer processes.

3.3. Electrochemical sensing using the rGO/SWCNT composite film

To demonstrate the enhanced electrochemical performance of the modified GCE, we selected H_2O_2 (an essential mediator in food, pharmaceutical, clinical, industrial, and environmental analyses, and also an important product of oxidized-enzymes) and NADH (a cofactor for dehydrogenase enzymes, important in the electron transfer chain of biological systems, and needed to

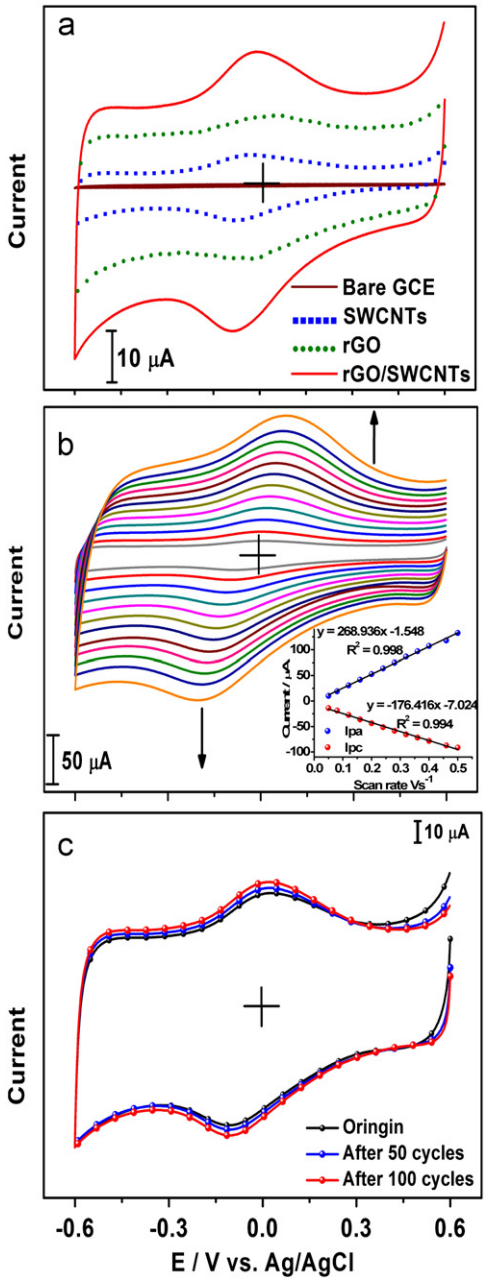

Fig. 3. Cyclic voltammogram of bare GCE and GCEs modified with SWCNTs, rGO, and rGO/SWCNT composite. (a) CV traces of bare GCE and GCEs modified with SWCNTs, rGO, and rGO/SWCNT composite films in PBS (pH 7.0); potential scan between +0.6 and −0.6 V; scan rate: 20 mV s^{-1}. (b) CV traces of the GCE modified with the rGO/SWCNT composite film. in N_2-saturated PBS at scan rates (from inner to outer) of 20, 80, 120, 160, 200, 240, 280, 420, 460, and 500 mV s^{-1}. Inset: Peak currents (I_{pa} and I_{pc}) plotted with respect to the scan rate. (c) After 100 continuous scan cycles, the rGO–SWCNT composite is stable and good adhesion to the surface.

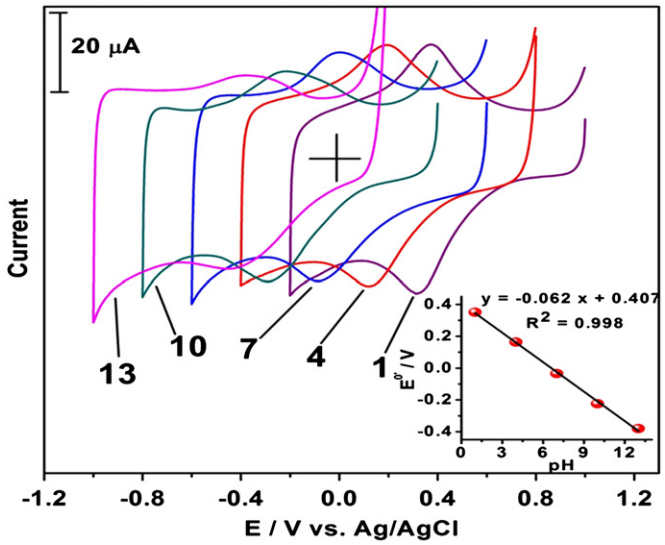

Fig. 4. CV traces of the rGO/SWCNT composite film prepared in PBS buffer (pH 7.0) and then transferred to solutions at various values of pH; scan rate: 20 mV s^{-1}. Inset: Formal potential plotted with respect to pH (1–13); the slope (−62 mV pH^{-1}) is close to that expected from the Nernst equation for an equal number of electron and proton transfer processes.

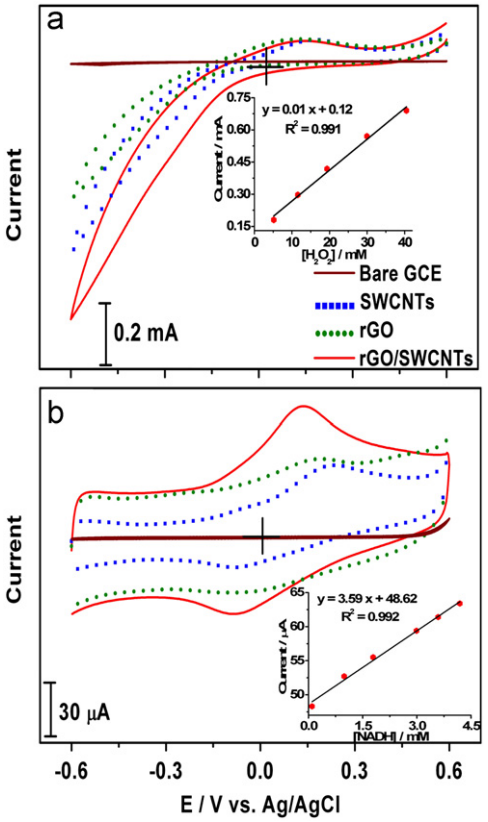

Fig. 5. CV traces of (a) H_2O_2 (40 mM) and (b) NADH (4 mM) at GCEs modified with SWCNT, rGO, and rGO/SWCNT composite films in PBS at 50 mV s^{-1}. Insets: Peak currents plotted with respect to H_2O_2 (NADH) concentration at the rGO/SWCNT composite film.

develop amperometric biosensors for substrates of NAD^+-dependent dehydrogenases) as analytes.

3.3.1. *Electrochemical reduction of H_2O_2 at the rGO/SWCNT electrode*

Fig. 5 presents the electrocatalytic reduction of H_2O_2 (40 mM) at the bare GCE and at GCEs modified with rGO, SWCNT, and rGO/SWCNT composite films, recorded at a scan rate of 100 mV s^{-1}. The CV trace for the rGO/SWCNT–modified electrode exhibits a reversible redox couple in absence of H_2O_2, with a new growth reduction peak appearing after the addition of H_2O_2. In electrocatalytic experiments, an increase in the concentration of the analyte provided a linear increase in the reduction peak current of H_2O_2. The reduction peak current of the rGO/SWCNT–modified

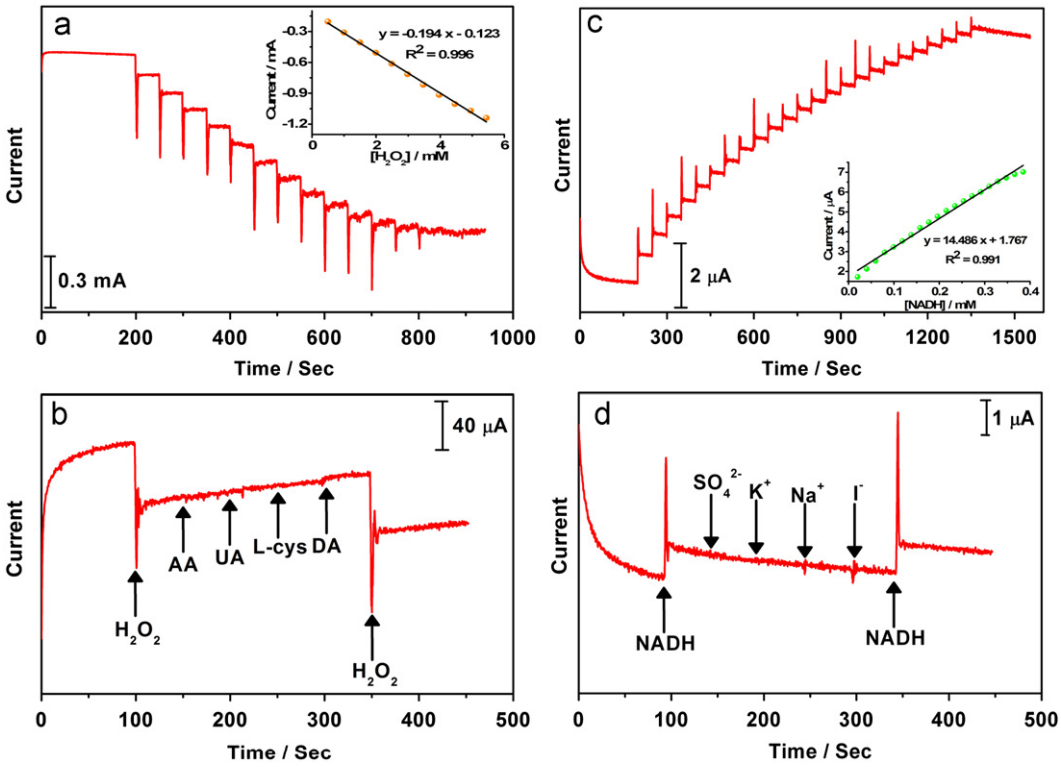

Fig. 6. The amperometric *i*–*t* responses and interference test toward the H_2O_2 and NADH detection. (a) *i*–*t* Curve data for the rGO/SWCNT composite film in PBS (at 1200 rpm and potential of $^{-}0.5$ V) in the presence of H_2O_2 at concentrations from 0.5 to 5.0 M. Inset: Current plotted with respect to the concentration of H_2O_2, obtained using the *i*–*t* curve at the rGO/SWCNT composite film. (b) Interference tests at the GCE modified with the rGO/SWCNT film after successive additions of solutions containing AA, DA, UA, and L-cys into continuously stirred N_2-saturated PBS. (c) Amperometric *i*–*t* responses at a GCE modified with the rGO/SWCNT film after successive additions of NADH (0.02–0.4 mM) into N_2-saturated PBS (applied potential: 0.1 V). Inset: Linear dependence of the peak current with respect to the concentration of NADH. (d) Interference of the amperometric response of the rGO/SWCNTs film in stirred PBS (pH 7.0) after injection of SO_4^{2-}, Na^+, K^+, and I^-, respectively.

electrode increased relative to those of the rGO- and SWCNT-only modified electrodes, indicating that the rGO/SWNCT composite had favorable catalytic ability for H_2O_2.

We used the amperometric response toward the addition of analyte to study the electrocatalytic reduction of H_2O_2 by the rGO/SWCNT–modified electrode [Fig. 6(a)]. The applied potential was set at -0.5 V with an electrode rotation speed of 1200 rpm; the amperometric response of the rGO/SWCNT–modified electrode was tested as a blank for an initial period of 200 s. After sequential addition of 0.5 M H_2O_2 at 50 s intervals, we could determine the correlative amperometric response of the rGO/SWNCT–modified electrode. The system exhibited good linearity between the reduction current and the concentration of H_2O_2 in the range from 0.5 to 5.0 M. The inset to Fig. 6(a) reveals a sensitivity of 2732.4 μA mM^{-1} cm^{-2} and a limit of detection (LOD) of 1.3 μM, based on a signal-to-noise (S/N) ratio of 3. Moreover, the rGO/SWCNT–modified electrode exhibited a very high selectivity for detecting H_2O_2: addition of 0.1 M AA, UA, or L-cys or 0.001 M DA did not interfere with the detection of 0.5 M H_2O_2 (Fig. 6(b)). The rGO/SWCNT–modified electrode also exhibited good long-term stability toward H_2O_2 detection, with the current response maintaining approximately 90% of its initial value after 1 month.

3.3.2. *Electrochemical oxidation of NADH by rGO/SWCNT electrodes*

We used CV to investigate the electrocatalytic oxidation of NADH on different electrodes (Fig. 5(b)). We tested the electrodes modified with individual and rGO/SWCNT composite films with NADH up to a concentration of 4 mM. The peak current for NADH oxidation at the rGO/SWCNT composite film was greater than those of the corresponding pristine films; the oxidation current was linear upon varying the concentration of the analyte. Moreover, the peak potential for NADH oxidation shifted from 0.18 and 0.25 V for the rGO and SWCNT films, respectively, to 0.13 V for the rGO/SWCNT–modified electrode. The decrease in the overvoltage at the rGO/SWCNT–modified electrode allowed the detection of NADH at lower potentials.

Fig. 6(c) displays the amperometric response at 0.1 V, with an electrode rotation speed of 1200 rpm, for the rGO/SWCNT–modified electrode after the successive addition of 0.4 mM NADH. This electrode responded very quickly to the addition of NADH. After an initial period of 200 s, the amperometric response was set as the blank; with the addition of 10 mM NADH, the amperometric response of the rGO/SWCNT–modified electrode was measured. The inset to Fig. 6(c) reveals a good relationship between the response current and the concentration of NADH in the range from 0.02 to 0.4 mM. The sensitivity at the rGO/SWNCT–modified electrode was 204 μA mM^{-1} cm^{-2} and the LOD of NADH was 0.078 μM ($S/N=3$). Thus, the rGO/SWCNT–modified electrode exhibited a high electrochemical response for the detection of NADH—a desirable feature for effective electrochemical sensors. From an interference test, Fig. 6(d) reveals that the addition of 0.1 M SO_4^{2-}, Na^+, K^+, or I^- did not interfere significantly with the detection of NADH, indicating that this system has high selectivity toward NADH.

4. Conclusions

We have developed a novel composite material, comprising SWCNTs and rGO, that provides stable aqueous solutions of SWCNTs for deposition onto GCE surfaces. These hybrid films were readily fabricated with high reproducibility and good stability. TEM, SEM,

and AFM imaging revealed that the SWCNTs could be disentangled through strong π–π interactions with the rGO. The rGO/SWCNT films exhibited good catalytic activity toward analytes (H_2O_2, NADH) and a detail study about interaction between analyte and the rGO/SWCNTs film. From CV and *i*–*t* curves, we characterized the rGO/SWCNT composite films both qualitatively and quantitatively, providing a simple and novel method for the development of voltammetric and amperometric sensors.

Acknowledgment

We thank the National Science Council of Taiwan and Academia Sinica, Taiwan, for financial support.

References

Abbaspour, A., Noori, A., 2011. Biosensors and Bioelectronics 26, 4674–4680.
Callegari, A., Cosnier, S., Marcaccio, M., Paolucci, D., Paolucci, F., Georgakilas, V., Tagmatarchis, N., Văızquez, E., Prato, M., 2004. Journal of Materials Chemistry 14, 807–810.
Chen, S.M., Periasamy, A.P., Ho, Y.H., 2011. Biosensors and Bioelectronics 29, 151–158.
Chena, K.J., Pillai, K.C., Rick, J., Pan, C.J., Wang, S.H., Liu, C.C., Hwang, B.J., 2012. Biosensors and Bioelectronics 33, 120–127.
Cote, L.J., Kim, F., Huang, J.X., 2009. Journal of the American Chemical Society 131, 1043–1049.
Daniel, S., Rao, T.P., Rao, K.S., Rani, S.U., Naidu, G.R.K., Lee, H.Y., Kawai, T., 2007. Sensors and Actuators B 122, 672–682.
Deng, C., Qu, F., Lu, H., Yang, M., 2011. Biosensors and Bioelectronics 26, 4810–4814.
Dey, R.S., Raj, C.R., 2010. Journal of Physical Chemistry C 114, 21427–21433.
Ge, S., Yan, M., Lu, J., Zhang, M., Yu, F., Yu, J., Song, X., Yu, S., 2012. Biosensors and Bioelectronics 31, 49–54.
Geim, A.K., Novoselov, K.S., 2007. Nature Materials 6, 183–191.
Gilje, S., Han, S., Wang, M., Wang, K.L., Kaner, R.B., 2007. Nano Letters 7, 3394–3398.
Guldi, D.M., Rahman, G.M.A., Zerbetto, F., Prato, M., 2005. Accounts of Chemical Research 38, 871–878.
Guo, S., Wu, X., Zhou, J., Wang, J., Yang, B., Ye, B., 2011. Journal of Electroanalytical Chemistry 655, 45–49.
Huang, J.H., Fang, J.H., Liu, C.C., Chu, C.W., 2010. ACS Nano 5, 6262–6271.
Hummers, W.S., Offeman, R.E., 1958. Journal of the American Chemical Society 80, 1339 1339.
Karyakin, A.A., Karyakina, E.E., Schmidt, H.L., 1999. Electroanalysis 11, 149–155.
Kim, F., Cote, L.J., Huang, J.X., 2010. Advanced Materials 22, 1954–1958.
Kruusenberg, I., Alexeyeva, N., Tammeveski, K., 2009. Carbon 47, 651–658.
Leng, C., Wu, J., Xu, Q., Lai, G., Jua, H., Yan, F., 2011. Biosensors and Bioelectronics 27, 71–76.
Li, Y., Umasankar, Y., Chen, S.M., 2009. Talanta 79, 486–492.
Lin, Y., Taylor, S., Li, H.P., Fernando, K.A.S., Qu, L.W., Wang, W., Gu, L.R., Zhou, B., Sun, Y.P., 2004. Journal of Materials Chemistry 14, 527–541.
Manjunatha, R., Nagaraju, D.H., Suresh, G.S., Melo, J.S., D'Souza, S.F., Venkatesha, T.V., 2011. Electrochimica Acta 56, 6619–6627.
Mitzi, D.B., Copel, M., Chey, S.J., 2005. Advanced Materials 17, 1285–1289.
Parpia, J.M., Craighead, H.G., McEuen, P.L., 2007. Science 315, 490–493.
Rubianes, M.D., Rivas, G.A., 2007. Electrochemistry Communications 9, 480–484.
Safavia, A., Farjamia, F., 2011. Biosensors and Bioelectronics 26, 2547–2552.
Schedin, F., Geim, A.K., Morozov, S.V., Hill, E.W., Blake, P., Katsnelson, M.I., Novoselov, K.S., 2007. Nature Materials 6, 652–655.
Si, P., Kannan, P., Guo, L., Son, H., Kim, D.H., 2011. Biosensors and Bioelectronics 26, 3845–3851.
Sun, Y.Y., Ren, Q., Liu, X., Zhao, S., Qin, Y., 2012. Biosensors and Bioelectronics 39, 289–295.
Tung, V.C., Chen, L.M., Allen, M.J., Wassei, J.K., Nelson, K., Kaner, R.B., Yang, Y., 2009. Nano Letters 9, 1949–1955.
Tung, V.C., Huang, J.H., Tevis, I., Kim, F., Kim, J., Chu, C.W., Stupp, S.I., Huang, J.X., 2011. Journal of the American Chemical Society 133, 4940–4947.
Wang, J., Kawde, A.N., Jan, M.R., 2004. Biosensors and Bioelectronics 20, 995–1000.
Yang, K., Zhang, C.Y., 2011. Biosensors and Bioelectronics 28, 257–262.
You, J.M., Jeong, Y.N., Ahmed, M.S., Kim, S.K., Choi, H.C., Jeon, S., 2011. Biosensors and Bioelectronics 26, 2287–2291.
Zhu, L., Zhai, J., Yang, R., Tian, C., Guo, L., 2007. Biosensors and Bioelectronics 22, 2768–2773.